An Adaptive Neuro-Fuzzy Controller for Vibration Suppression of Flexible Structures

Adam Genno, *Student Member, IEEE*, Wilson Wang, *Senior Member, IEEE*

***Abstract*—Neuro-fuzzy (NF) controllers are useful in a wide range of industrial applications and their robust capability can be provided by proper training methods. In this article an adaptive NF controller is developed to suppress the vibration of perturbed flexible structures. A new training technique based on the bisection particle swarm optimization (BPSO) algorithm is proposed to optimize the NF controller parameters recursively. To reduce additional vibration induced by controller response to nonlinearities in the steady-state solution space, a fuzzy boundary function is suggested to shape the control signal and reduce the induced vibrations from the control action. The parameters related to output suppression are optimized simultaneously during recursive NF system training. Experiments are provided to validate the effectiveness of the adaptive NF control technique and the BPSO training method.**

***Index Terms*—Neuro-fuzzy (NF) systems, parameter training, adaptive control, hybrid training, flexible structures, vibration suppression.**

I. Introduction

FLEXIBLE structures are more and more widely used in various engineering applications such as robots, mechanical structures, and aircrafts, due to their increased flexibility and reduced weight. From a control perspective, both the increased flexibility and reduced weight present more challenges in structure vibration control. Increasing a system's flexibility introduces additional degrees of freedom in the form of torsional and elastic deformation [1]. Thus, flexible structures represent classical underactuated systems, making many traditional control methods ineffective. The reduced weight can introduce flexible modes into the system, which will result in additional vibrations in the steady state solution space [2, 3]. In system control practice, these vibrations could degrade control performance with increased convergence time and reduced precision attainable by the controller, or even control instability.

Several control strategies have been proposed in literature to deal with the nonlinear dynamics of flexible structures. Classical control methods such as PD and PID controls have been used for vibration suppression in flexible structures [4-6]. However, these control techniques utilize fixed control gains that are difficult to tune for satisfactory performance especially in noisy plant environments. More advanced control techniques have been suggested to address the issue of nonlinear system dynamics such as sliding mode control [7-9], adaptive control [10], and dynamic surface control [11, 12]. Among these techniques, sliding mode control is more widely utilized due to its simplicity and resistance to changing system dynamics. However, sliding mode control is susceptible to the chattering phenomenon, and control actions in response to nonlinearities can induce additional vibrations into the solution space [13].

In the last decade, intelligent controllers have been proposed in literature for control applications using soft computing tools such as fuzzy logic (FL) [14-16], and neural networks (NN) [17-19]. FL systems have approximation capabilities in using fuzzy If-Then rules, but are rigid in structure and lack the learning capability required to adapt to changing system dynamics. Conversely, although NN systems have adequate learning capabilities, their reasoning is usually in a black-box form; as a result, developed control reasoning is complex and difficult to interpret for knowledge processing. Neuro-fuzzy (NF) controllers are a hybrid class combining FL and NN systems to circumvent their respective shortcomings [20].

The performance of NF controllers can be improved by using proper training algorithms. A hybrid strategy is generally used to train linear and nonlinear NF parameters to improve training efficiency. One of the most frequently utilized methods is the combination of least-squares estimation (LSE) and gradient-descent (GD) to optimize the linear and nonlinear parameters, respectively [21]. However, these derivative-based methods are usually sensitive to initial conditions and are prone to trapping in local minima. To address this shortcoming, several heuristic optimization algorithms have been proposed in literature to improve convergence [22-25]; however, these methods are usually computationally expensive, making them difficult to implement in real-time control applications.

To tackle the aforementioned problems, an adaptive NF controller is developed in this work for the control of perturbed flexible structures. It is new in the following aspects:

1) In the NF controller, dynamic output suppression is employed to reduce the nonlinearly induced vibrations.
2) A new training algorithm based on bisection particle swarm optimization (BPSO) is proposed to optimize the non-linear NF controller parameters more effectively.
3) The workstation is improved to reduce the prevalence of noise in the experimental data.

The rest of this article is organized as follows. Section II describes the experimental setup and the dynamic model of the flexible structure. Section III discusses the proposed NF controller and hybrid training technique. The effectiveness of the developed control technology is verified in Section IV.

II. System Modeling

A. Experimental Setup

Fig. 1 shows the test apparatus used in this work, which consists of a flexible beam that is clamped at one end and free at the other. Attached to the free end of the flexible beam is a DC motor that drives a rigid rotary dual-bar linkage through

gear trains with a total gearbox ratio of 70. An optical-shaft encoder (4096 counts per revolution) is used to measure the angular position of the rigid rotary bar in a quadrature mode. The deflection of the flexible beam is measured by a dual grid half bridge strain gauge secured to the bottom of the beam. The analog deflection signal is measured through a signal conditioning board with a calibration of a 1-inch deflection of the tip of the flexible beam corresponding to a 1 V signal.

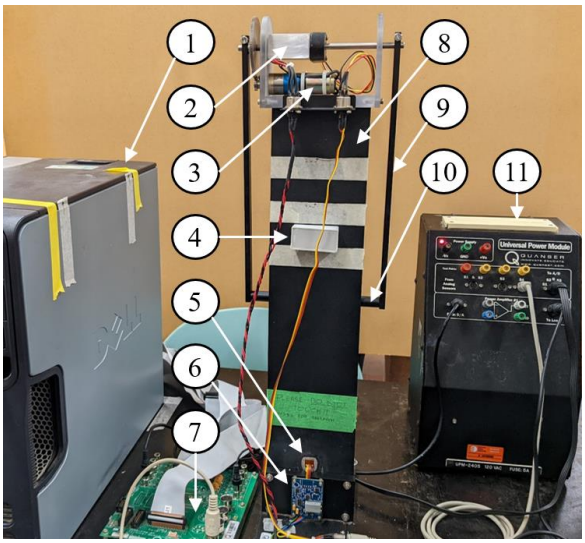

Fig. 1. The experimental setup: (1)-computer, (2)-encoder, (3)-motor, (4)-extra mass blocks, (5)-strain gauges, (6)-signal conditioning board, (7)-terminal board, (8)- flexible beam, (9)-rigid bars, (10)-cross beam. (11)-power amplifier.

B. A New Signal Conditioning Board

Fig. 2 shows the updated signal conditioning board is designed and installed to the test apparatus to improve the signal-to-noise ratio of the vibration signal measured from the strain gauge. Flexible beam deflections change the electrical resistance of the strain gauge, which changes the voltage measured across the leads of the strain gauge. Two amplifiers are used to boost voltage signal. Voltage to the conditioning board is supplied from the operational; the positive power regulator provides sufficient voltage for board operation. Two potentiometers are utilized to fine tune circuit output and allow for adjustment of the output signal gain and offset. The updated board incorporates decoupling capacitors to reduce the noise in the measured signal and voltage references for improved data resolution [26].

C. System Model

The flexible beam illustrated in Fig. 1 can be modeled as

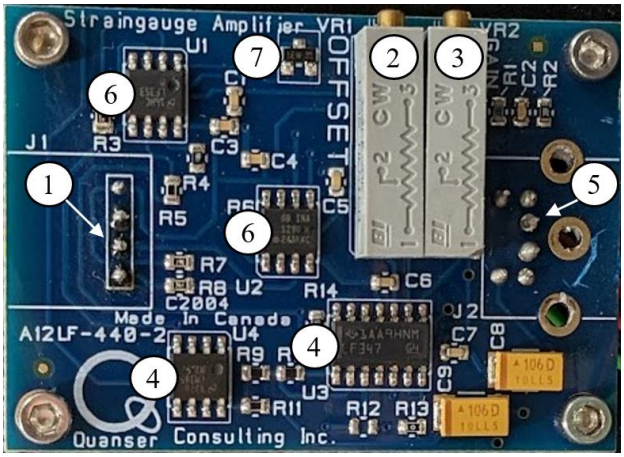

Fig. 2. The updated signal conditioning board: (1)-strain gauge signal input, (2)-offset adjustment potentiometer, (3)-gain adjustment potentiometer, (4)-operational amplifiers, (5)-conditioned signal output, (6)-voltage references, (7)-voltage regulator.

shown in Fig. 3. The system dynamics can be described by the following motion equations:

$$(m_b + m_p)\ddot{x}_b + m_p l_p \cos(\theta_p)\ddot{\theta}_p - m_p l_p \sin(\theta_p)\dot{\theta}_p{}^2 + k_s x_b = 0 \tag{1}$$

$$(J_p + m_p l_p{}^2)\ddot{\theta}_p + m_p l_p \cos(\theta_p)\ddot{x}_b - m_p l_p g \sin(\theta_p) = \frac{\eta_g K_g \eta_m k_t}{R_m}(V_m - K_g k_m \dot{\theta}_p) \tag{2}$$

where x_b is the deflection of the flexible beam from the undeflected vertical position in centimeters; θ_p is the angular position of the rigid bar in rad; l_p is the length of the rigid rotary bar; m_b and m_p are the respective masses of the motor fixture and cross beam; and V_m is generated control signal. Table I summaries the related parameters and their descriptions.

III. Design of the Neuro-Fuzzy Controller

A. Neuro-Fuzzy Controller Architecture

An adaptive NF controller will be developed to suppress the vibration exhibited by the flexible beam. Consider n input variables $\{x_1, x_2, \ldots, x_n\}$ and one output z, the fuzzy rules can be represented with the following general form [27]:

$$\Re_j : If\ (x_1\ is\ A_1^j)\ and\ (x_2\ is\ A_2^j)...and\ (x_n\ is\ A_n^j)\ then\ (z_j = b_0^j + b_0^j x_1 + ... + b_n^j x_n) \tag{3}$$

where $A_i{}^j$ is a membership function (MF); i = 1, 2, …, n; j = 1, 2, …, J; J is the total number of MF for each input, j is the fuzzy rules; and $b_n{}^j$ are linear consequent constants.

Consider four inputs (n = 4): $\{x_1, x_2, x_3, x_4\}$ corresponding to four respective system states: $\{x_b, \theta_p, \dot{x}_b, \dot{\theta}_p\}$. The developed NF system will have 16 rules or J = 16. Fig. 4 shows the NF

system network architecture. It has five layers with unity link weights. The inputs are fuzzified in Layer

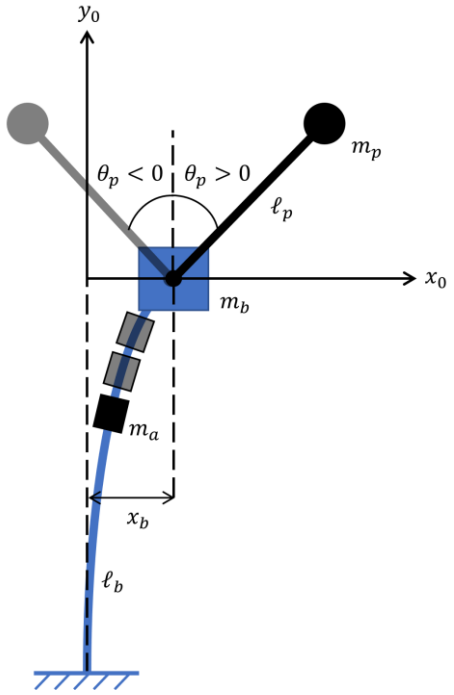

Fig. 3. Two-dimensional model of the experimental setup.

TABLE I. FLEXIBLE STRUCTURE SPECIFICATIONS

Description	Symbol	Value/Unit
Mass of motor fixture	m_b	0.60 kg
Mass of cross beam	m_p	0.05 kg
Mass of addl. blocks	m_a	0.15 kg
Flexible beam length	l_b	0.44 m
Rigid rotary bar length	l_p	0.292 m
Mass moment of inertia	J_p	4.09E-3 kg/m^3
Gravitational accel.	g	9.81 m/s^2
Gearbox efficiency	η_g	0.90
Total gearbox ratio	K_g	70
Motor efficiency	η_m	0.69
Motor torque constant	k_t	7.68E-3 N.m
Motor armature resist.	R_m	2.6 Ω
Nominal motor voltage	V_m	6 V
Back-emf constant	k_m	7.68E-3 V/(rad/s)

1 using two sigmoid membership functions (MFs), small (negative large) and large (positive large), with the following form:

$$\mu_{A_i^j}(x_i) = \frac{1}{1+\exp[-a_i^j(x_i - c_i^j)]} \tag{4}$$

where x_i corresponds to an input from $\{x_1, x_2, x_3, x_4\}$; a_i^j and c_i^j represent nonlinear parameters, n = 1, 2, ..., 8, for positive large and for negative large correspond to $a_i^j > 0$ and $a_i^j < 0$, respectively.

The firing strength of each fuzzy rule is computed in Layer 2. If a product T-norm for each fuzzy rule, then:

$$w_j = \prod_{i=1}^{4} \mu_{A_i^j}(x_i) \tag{5}$$

where j = 1, 2, ..., 16.
The normalized firing strength is computed in Layer 3, or:

$$N_j = \frac{w_j}{\sum_{j=1}^{16} w_j} \tag{6}$$

j = 1, 2, ..., 16 is the total number of fuzzy rules. If centroid defuzzification is performed in Layer 4, the control output z will be:

$$z = \sum_{j=1}^{16} N_j (b_0^j + b_1^j x_1 + ... + b_4^j x_4) \tag{7}$$

where $b_0^j, b_1^j, ..., b_4^j$ are consequent linear parameters.

The linear and nonlinear parameters of the NF controller are optimized using the hybrid training technique outlined in Section IV.

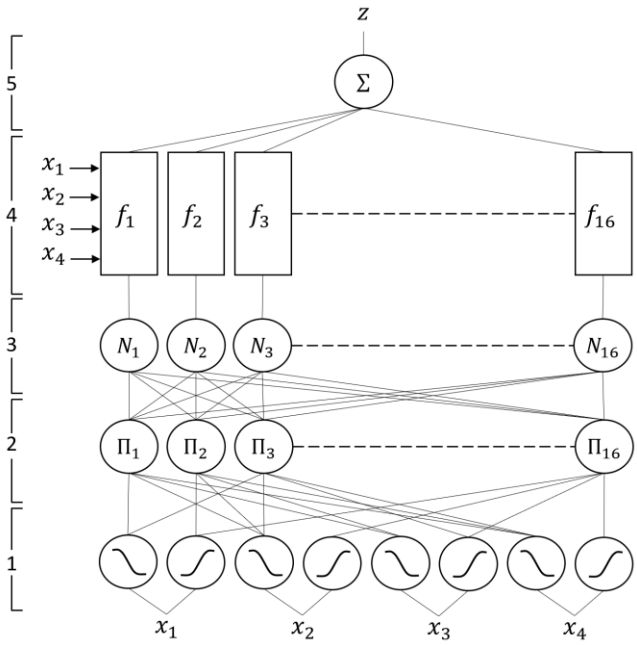

Fig. 4. Architecture of the NF controller (Dr. Wang to replace)

B. NF Output Suppression

To facilitate convergence of the NF control, the vibration suppression on the flexible beam will take a restoring force on the flexible structure to facilitate equilibrium. The magnitude of the restoring control force is directly proportional to the deflection of the flexible structure [28] (did you mean to remove this reference? If so we need to renumber after this point). For a mass-spring-damper model with a discrete mass node, the restoring force can be formulated to interact the spring and damping forces:

$$f_r(x, \dot{x}) = kx + d\dot{x} \tag{8}$$

where k and d are the related system stiffness and damping coefficients.

From systematic experimental investigation, it is found that extra variations in control action exist when the system state is close to the origin, suggesting a dependence on more than position and velocity. These results were also present in literature where it was found that the restoring force of flexible structures exhibited nonlinear characteristics at higher velocities [29]. To accommodate this effect without further system parameterization, a simple dynamic output suppression technique is proposed to limit the control action of the controller for input ranges where variations are more prevalent.

Consider the following Gaussian MF:

$$\mu_{A_5^j}(x_i) = \exp\left[-\frac{1}{2}\frac{(x_5 - c)^2}{\lambda\,\sigma^2}\right] \tag{9}$$

where x_5 is the NF input corresponding to flexible beam deflection, c is the center of the MF and σ is the standard deviation. The parameter λ is the deflection overshoot or undershoot are defined as the first and second deflection minima in response to system perturbation.

Consider the complement in Eq. (10):

$$\mu_{A_6^j}(x_5) = 1 - \mu_{A_5^j}(x_5) \tag{10}$$

A continuous fuzzy boundary function can be formed by utilizing the max *S*-norm (*T*-conorm) of the fuzzy sets E_1 and its complement:

$$\mu_{A_7^j}(x_5) = \mu_{A_5^j}(x_5) \vee \mu_{A_6^j}(x_5) \tag{11}$$

By concurrently updating the fuzzy boundary function during NF parameter training, the range of beam deflection inputs that correspond to a limited controller response can be adjusted dynamically. The width of the range of inputs will be narrower when the difference between the deflection overshoot and undershoot is smaller. Conversely, the range will be wider when the difference is larger. Fig. 5 shows the MFs of E_1 and E_2 and the associated boundary function E_3 .

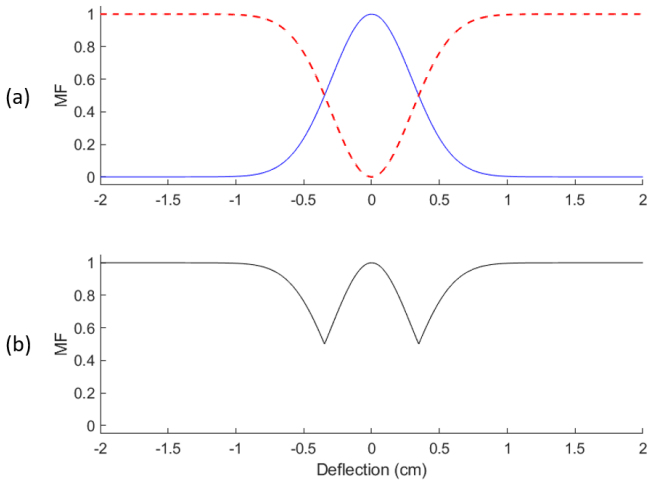

Fig. 5.(a) Plot of fuzzy MFs A_5 (solid) and A_6 (dashed line). (b) Fuzzy boundary function A_7.

C. BPSO System Training

The linear and nonlinear NF parameters are optimized by a novel hybrid training technique based on least-squares estimator (LSE) and the proposed BPSO. System training is performed in two passes for all training data pairs propagated through the NF controller. In general, the training data pairs should be at least 5-times the number of linear data points to be optimized [27]. In the forward pass the nonlinear parameters are fixed, and the linear parameters are updated using the LSE. In the backward pass the linear parameters are fixed, and the nonlinear parameters search area is updated using BPSO.

1) BPSO-based Nonlinear Parameter Training

Although heuristic training algorithms can improve global minimums in optimization, they are computationally expensive. To address this issue, the computationally efficient bisection method is integrated in particle swarm optimization to incrementally optimize the nonlinear system parameters. The algorithm will span a solution space across each nonlinear parameter to be optimized. The upper boundary $\mathcal{B}_u$ and lower boundary $\mathcal{B}_l$ of the solution space is initialized as follows:

$$\mathrm{B}_{u,0} = b_0 + \delta \tag{12}$$

$$\mathrm{B}_{l,0} = b_0 - \delta \tag{13}$$

where b_0 is a generalized variable representing the initial value of the nonlinear parameter to be optimized; δ is a parameter representing the width of one-half of the solution space.

In this work, the width will be based on the product of a random value γ, and a percentage of the magnitude of the initial nonlinear parameter:

$$\delta = \mathrm{rand}(\gamma \cdot b_0) \tag{14}$$

For each propagated training data pair, the NF system output is concurrently computed for upper boundary particle y_u and the lower boundary particle y_l. The respective error of each particle is calculated by comparing it to the desired NF output y_d:

$$\varepsilon_u = |y_u - y_d| \tag{15}$$

$$\varepsilon_l = |y_l - y_d| \tag{16}$$

Based on the calculated error, the corresponding boundary particle is bisected as follows:

$$\mathrm{B}_{u,i+1} = \begin{cases} \mathrm{B}_{u,i} - \left|\dfrac{\mathrm{B}_{u,i} - \mathrm{B}_{l,i}}{2}\right| & \text{if } \varepsilon_l \geq \varepsilon_u \\ \mathrm{B}_{u,i} & \text{otherwise} \end{cases} \tag{17}$$

$$\mathrm{B}_{l,i+1} = \begin{cases} \mathrm{B}_{u,i} - \left|\dfrac{\mathrm{B}_{u,i} - \mathrm{B}_{l,i}}{2}\right| & \text{if } \varepsilon_l < \varepsilon_u \\ \mathrm{B}_{l,i} & \text{otherwise} \end{cases} \tag{18}$$

This process is repeated iteratively until the difference between boundary particles becomes sufficiently small.

$$\left|\mathrm{B}_{u,i}-\mathrm{B}_{l,i}\right|<\varepsilon_{\min} \tag{19}$$

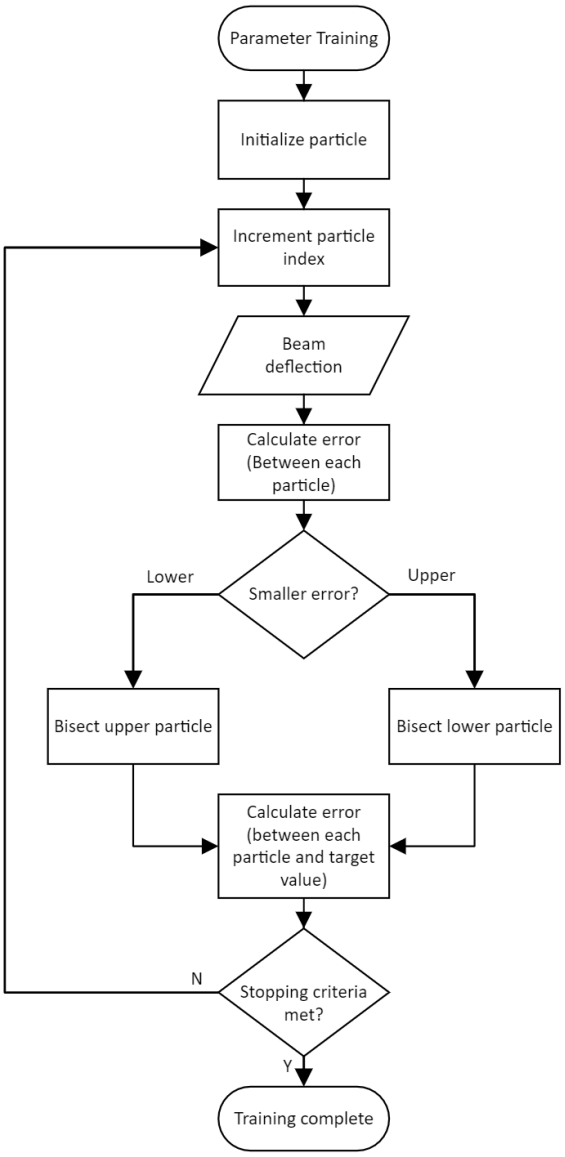

Fig. 6. Flowchart of the nonlinear parameter training algorithm methodology. (Dr. Wang to replace)

In experimental procedures, the stopping criteria is selected as $\varepsilon_{min}=10^{-6}$ by trial and errors This can ensure training iterations are performed properly, and training operations do not immediately conclude in instances where δ is small. A flowchart indicating the training algorithm methodology is illustrated in Fig. 6.

2) LSE for Linear Parameter Training

The LSE is used to optimize the linear parameters of the proposed NF controller, by minimizing the objective function or minimizing the errors between the desired system outputs and calculated system outputs. Consider the outputs generated by a NF controller:

$$\theta_1 f_1(\boldsymbol{u})+\theta_2 f_2(\boldsymbol{u})+\ldots++\theta_n f_n(\boldsymbol{u})=\mathrm{y} \tag{20}$$

where $\boldsymbol{u}$ are the NF controller inputs $\{x_1, x_2, \ldots, x_n\}$; $\boldsymbol{\theta}=\{\theta_1, \theta_2, \ldots, \theta_n\}$ (Not correct. The numbers of inputs and parameters are usually different) correspond to the unknown linear parameters; $\{z_1, z_2, \ldots, z_n\}$ are the nodal outputs from Layer 4 of the NF controller as illustrated in Fig. 4; and z is the NF controller output. A matrix representation can be represented as:

$$\begin{bmatrix} f_1(\boldsymbol{u}_1) & f_2(\boldsymbol{u}_1) & \cdots & f_j(\boldsymbol{u}_1) \\ f_1(\boldsymbol{u}_2) & f_2(\boldsymbol{u}_2) & \cdots & f_j(\boldsymbol{u}_2) \\ \vdots & \vdots & & \vdots \\ f_1(\boldsymbol{u}_m) & f_2(\boldsymbol{u}_m) & \cdots & f_j(\boldsymbol{u}_m) \end{bmatrix} \begin{bmatrix} \theta_1 \\ \theta_2 \\ \vdots \\ \theta_j \end{bmatrix} = \begin{bmatrix} y_1 \\ y_2 \\ \vdots \\ y_m \end{bmatrix} \tag{21}$$

where $\boldsymbol{u_j}$ are the NF controller inputs corresponding to the m^{th} training data pair for m = 1, 2, ..., M; M is the number of training data pairs, and j is the number of fuzzy rules (does this make sense instead?) to be optimized. Eq. (23) can further be simplified as:

$$\boldsymbol{A\theta}=\boldsymbol{y} \tag{22}$$

Thus, the error between the desired and calculated NF outputs can be written as:

$$\boldsymbol{e}=\boldsymbol{y}-\boldsymbol{A\theta} \tag{23}$$

and the objective function can be written as:

$$E(\boldsymbol{\theta})=\frac{1}{2}\sum_{m=1}^{M}(y-\boldsymbol{a}_i^{\mathrm{T}}\boldsymbol{\theta})^2 \tag{24}$$

where a_i is row from matrix $\boldsymbol{A}$, as denoted by its subscript.

Minimizing the objective function in Eq. (26) with respect to the vector containing the linear parameters to be optimized yields the following expression:

$$\boldsymbol{\theta}=(\boldsymbol{A}^{\mathrm{T}}\boldsymbol{A})^{-1}\boldsymbol{A}^{\mathrm{T}}\boldsymbol{y} \tag{25}$$

IV. Experimental Results

To verify the effectiveness of the proposed controller andhybrid training technique, a series of experimental tests have been conducted. Each test begins with a "swing-up" procedure, where the rigid bar is balanced above the flexible beam until astable solution is achieved. Then, a time-limited voltage is provided to the DC motor to drive the rigid bar to perturb the flexible structure. A time-limited perturbation signal is used to accommodate variations in the initial deflection of the flexible structure. After applying the perturbation signal, the controller is activated to suppress the vibrations to achieve a steady state solution. To examine the effectiveness of the developed control system (Controller-4), three related controllers are utilized in this testing procedure as follows:

a) Controller-1: A classical fuzzy controller without system training.
b) Controller-2: The proposed NF controller, trained using a hybrid method with LSE and GD algorithm.
c) Controller-3: The proposed NF controller, trained using a hybrid method with LSE and the proposed BPSO.

d) Controller-4: The proposed NF controller with output suppression, trained using a hybrid method with LSE and the proposed BPSO.

A performance comparison is made between each controller based on overshoot, undershoot, and settling time. Overshoot and undershoot are calculated based on the deviation from the mean steady state solution. Settling time is determined by placing a boundary around the mean steady state solution and recording the last instance where the beam deflection crosses the boundary. For this experiment a total boundary width of 0.2 cm was selected to accommodate the high frequency vibrations that remain in the steady state solution space.

A comparison between Controller-1 and Controller-2 is made to assess the feasibility of using a NF controller (i.e., NF vs a general fuzzy control) to suppress the vibrations of the flexible structure. Both Controller-2 and Controller-3 have the identical NF structure; but the test is to examine the effectiveness of the proposed BPSO training method in Controller-3, with respect to the classical GD algorithm utilized in Controller-2 to optimize the nonlinear controller parameters. Both Controller-3 and Controller-4 are trained using the same hybrid training method; the comparison is to examine the effectiveness of the proposed output suppression technique used in Controller-4 to reduce the vibrations induced during controller response.

The deflection of the flexible beam during perturbation and control performance from the four tested controllers is shown in Fig.6. The related test results are summarized in Table II. Clearly, NF controllers (Controllers 2-4) outperform the classical fuzzy controller (Controller-1) due to proper system training. Although both Controller-2 and Controller-3 exhibit similar control characteristics, Controller-3 is able to achieve a reduction in settling time compared to Controller-2, due to the effective BPSO training strategy. On the other hand, Controller-4 performs even better than Controller-3 due to its efficient output suppression strategy in reducing overshoot, undershoot, settling time and the associated high frequency oscillations induced by control actions.

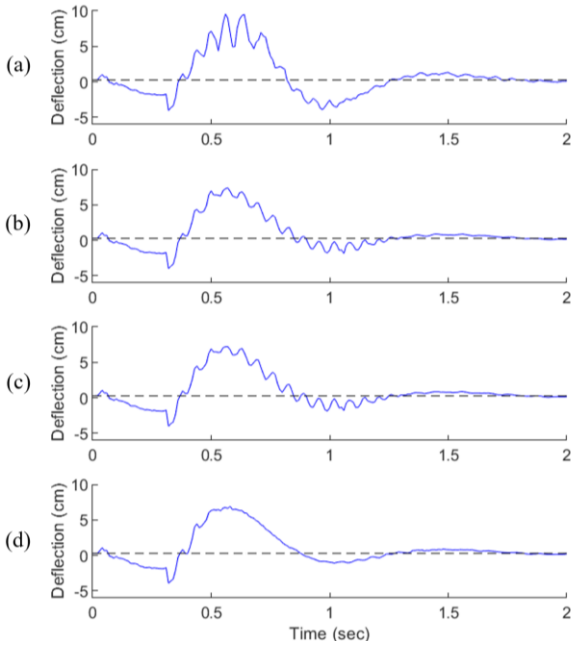

Fig. 6. Deflection of the flexible beam using each controller: (a) Controller-1, (b) Controller-2, (c) Controller-3, (d) Controller-4.

TABLE II. EXPERIMENTAL RESULTS –NO ADDITIONAL MASS

Controller	Overshoot (cm)	Undershoot (cm)	Settling Time (msec)
Controller-1	9.30	3.64	455
Controller-2	7.10	1.58	363
Controller-3	6.94	1.58	317
Controller-4	6.62	0.82	298

Extra magnetic mass blocks are placed at different locations along the flexible beam to simulate the variable system dynamics. This test demonstrates the adaptability of the controllers in response to dynamic loading. Each mass block weighs 50g; a pair of mass blocks is placed on the opposite sides of the beam in each test. The mass blocks are placed at one of three different locations, or zones, along the length of the flexible beam. Each zone is about 1 inch wide. Zone 1 begins 2 inches from the top of the flexible beam, and Zones 2 and 3 are located with an additional 2 inches downward, respectively.

Additional mass blocks are placed on Zone 1 of the flexible structure to simulate different beam dynamics. The performance of the related controllers is shown in Fig.7, and the results are summarized in Table III. Similar trends can be observed as with the no load case, or NF controllers (Controllers 2-4) perform better than the fuzzy controller

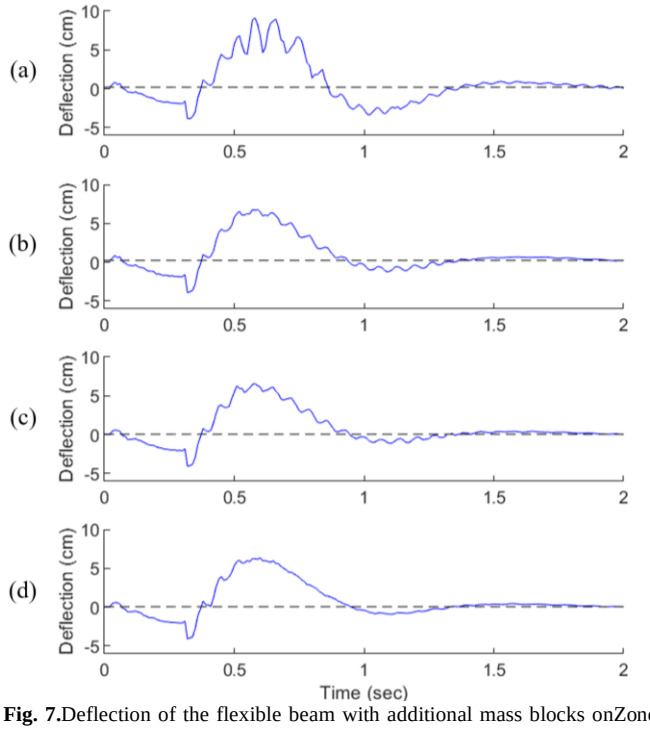

Fig. 7. Deflection of the flexible beam with additional mass blocks onZone 1 using different controllers: (a) Controller-1, (b) Controller-2, (c) Controller-3, (d) Controller-4.

TABLE III. EXPERIMENTAL RESULTS - ADDITIONAL MASS ON ZONE 1

Controller	Overshoot (cm)	Undershoot (cm)	Settling Time (msec)

	(cm)	(cm)	Time (msec)
Controller-1	8.93	3.19	238
Controller-2	6.56	1.02	237
Controller-3	6.50	1.07	214
Controller-4	6.30	0.85	190

(Controller-1) due to training operations. With respect to Controller-1, Controller-3 has a reduction in settling time with compared to Controller-2, due to the effective BPSO training that can recurrently update the nonlinear MF parameters and accommodate changing system dynamics. On the other hand, the developed Controller-4 outperforms other three controllers due to its superior high frequency oscillation suppression capability.

The mass blocks are placed to Zone 2 to simulate a different flexible beam dynamics. The performance of the related controllers is illustrated in Fig. 8, and the results are summarized in Table IV. Controllers 2-4 perform better than Controller 1 due to training operations. Compared to Controller-1, both Controller-2 and Controller-3 have a reduction in settling time. Controller-3 is able to achieve superior results compared to Controller-2 due to the recurrent optimization of the nonlinear parameters through BPSO training, but the results are less significant compared to the loading case where the mass blocks are placed on Zone 1. Controller-4 performs even better than Controller-3 by coupling the proposed output suppression technique with the proposed BPSO training technique. As a result, the prevalence of high frequency oscillations in the steady state space is reduced, andan improved reduction in settling time is achieved.

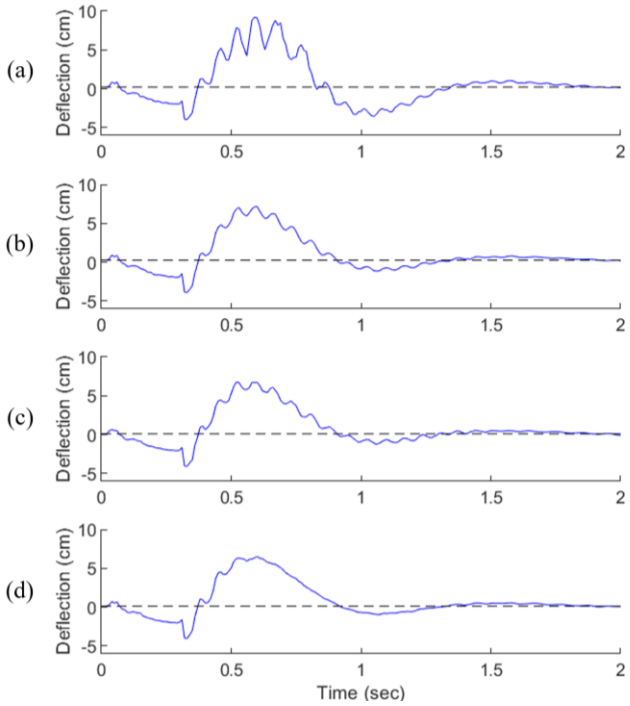

Fig. 8. Deflection of the flexible beam with additional mass blocks onZone2 using different controllers: (a) Controller-1, (b) Controller-2, (c) Controller-3, (d) Controller-4.

TABLE IV. EXPERIMENTAL RESULTS - ADDITIONAL MASS ON ZONE 2

Controller	Overshoot (cm)	Undershoot (cm)	Settling Time (msec)
Controller-1	8.99	3.33	272
Controller-2	6.98	1.01	225
Controller-3	6.66	1.13	222
Controller-4	6.42	0.83	213

The flexible beam dynamics are changed by moving the mass blocks to Zone 3. The performance of each controller is shown in Fig. 9, and the experimental results are summarized in Table V. Similar to other experimental procedures, training operations allow Controllers 2-4 to achieve better results compared to Controller-1. When compared to Controller-1, Controller-2 and Controller-3 can achieve a reduced settling time. Controller-3 outperforms Controller-2 by recursively updating the nonlinear NF MF parameters using the proposed BPSO method. Controller-4 achieves better results compared to Controller-3 by utilizing the proposed output suppression technique, which can reduce the high frequency oscillations induced by control actions.

V. CONCLUSION

This article explored the development of a new hybrid training technique, and an adaptive controller for vibration suppression in flexible structures. The new hybrid training technique utilizes a novel heuristic method to recursively optimize nonlinear parameters, allowing local minima to be

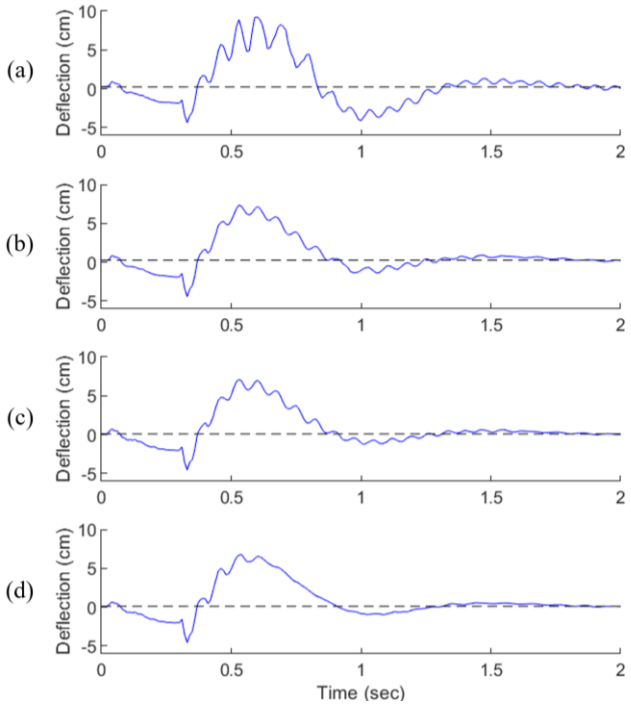

Fig. 9. Deflection of the flexible beam with additional mass blocks onZone3 using different controllers: (a) Controller-1, (b) Controller-2, (c) Controller-3, (d) Controller-4.

TABLE V. EXPERIMENTAL RESULTS - ADDITIONAL MASS ON ZONE 3

Controller	Overshoot (cm)	Undershoot (cm)	Settling Time (msec)

Controller-1	9.01	3.86	283
Controller-2	7.09	1.11	263
Controller-3	7.03	1.16	214
Controller-4	6.68	0.87	204

escaped. An updated controller with a fuzzy boundary function is utilized to suppress the control output during periods of nonlinear system response to reduce the prevalence of high frequency oscillations in the steady state solution space. Resistance to dynamic loading is demonstrated by placing additional mass blocks at specific locations along the length of the flexible beam.Test results have shown that the proposed hybrid training technique has some advantages over conventional techniques for all loading scenarios. Additional advantages are observed when the proposed hybrid training technique is used in combination with the proposed output suppression technique, demonstrating improved controller performance for vibration suppression applications.

REFERENCES

[1] H. Huang, G. Tang, H. Chen, L. Han, and D. Xie, “Dynamic modeling and vibration suppression for two-link underwater flexible manipulators,” *IEEE Access*, vol. 10, 2022.

[2] W. Zhu, Q. Zong and B. Tian, "Adaptive tracking and command shaped vibration control of flexible spacecraft," *IET Control. Theory Appl.*, vol. 13, no. 8, pp. 1121-1128, May 2019.

[3] C. F. Cutforth and L. Y. Pao, "Adaptive input shaping for maneuvering flexible structures," *Automatica*, vol. 40 no. 4, pp. 685-693, Apr. 2004.

[4] M. -A. Bégin, R. Poon and I. Hunter, "Streamlined tuning procedure for stable PID control of flexible-base manipulators," *IEEE Robot. Autom. Lett.*, vol. 6, no. 4, pp. 7413-7420, Oct. 2021.

[5] Y. Guo and M. E. A. Mohamed, "Speed control of direct current motor using ANFIS based hybrid P-I-D configuration controller," *IEEE Access*, vol. 8, pp. 125638-125647, 2020.

[6] Yunhiu Liu and Dong Sun, "Stabilizing a flexible beam handled by two manipulators via PD feedback," *IEEE Trans. Automat. Contr.*, vol. 45, no. 11, pp. 2159-2164, Nov. 2000.

[7] T. Long et al., "A vibration control method for hybrid-structured flexible manipulator based on sliding mode control and reinforcement learning," *IEEE Trans. Neural Netw. Learn. Syst.*, vol. 32, no. 2, pp. 841-852, Feb. 2021.

[8] K. Rsetam, Z. Cao and Z. Man, "Design of robust terminal sliding mode control for underactuated flexible joint robot,"*IEEE Trans. Syst. Man Cybern., Syst.*, vol. 52, no. 7, pp. 4272-4285, Jul. 2022.

[9] J. Li, J. Wang, H. Peng, Y. Hu and H. Su, "Fuzzy-torque approximation-enhanced sliding mode control for lateral stability of mobile robot," *IEEE Trans. Syst. Man Cybern. Syst.*, vol. 52, no. 4, pp. 2491-2500, Apr. 2022.

[10]Y. -J. Liu, S. Lu, S. Tong, X. Chen, C. L. P. Chen, and D. -J. Li "Adaptive control-based barrier Lyapunov functions for a class of stochastic nonlinear systems with full state constraints," *Automatica*, vol. 87, pp. 83-93, Jan. 2018.

[11]X. Xu and S. Xu, "Event-triggered adaptive neural tracking control of flexible-joint robot systems with input saturation," *IEEE Access*, vol. 10, pp. 43367-43375, 2022.

[12]S. Wang, H. Yu, J. Yu, J. Na and X. Ren, "Neural-network-cased adaptive funnel control for servo mechanisms with unknown dead-zone," *IEEE Trans. Cybern..*, vol. 50, no. 4, pp. 1383-1394, Apr. 2020.

[13]S. Wang, L. Tao, Q. Chen, J. Na and X. Ren, "USDE-based sliding mode control for servo mechanisms with unknown system dynamics," *IEEE/ASME Trans. Mechatronics*, vol. 25, no. 2, pp. 1056-1066, Apr. 2020.

[14]H. Li, L. Wang, H. Du and A. Boulkroune, "Adaptive fuzzy backstepping tracking control for strict-feedback systems with input delay," *IEEE Trans. Fuzzy Syst.*, vol. 25, no. 3, pp. 642-652, Jun. 2017.

[15]Z. Li, C.-Y. Su, L. Wang, Z. Chen and T. Chai, "Nonlinear disturbance observer-based control design for a robotic exoskeleton incorporating fuzzy approximation," *IEEE Trans. Ind. Electron.*, vol. 62, no. 9, pp. 5763-5775, Sep. 2015.

[16]L. Wan, Y. -J. Pan and H. Shen, "Improving synchronization performance of multiple Euler–Lagrange systems using nonsingular terminal sliding mode control with fuzzy logic," *IEEE/ASME Trans. Mechatronics*, vol. 27, no. 4, pp. 2312-2321, Aug. 2022.

[17]H.Gao, W. He, L. Zhang and C. Sun, "Neural-network control of a stand-alone tall building-like structure with an eccentric load: an experimental investigation," *IEEE Trans. on Cybern.*, vol. 52, no. 6, pp. 4083-4094, Jun. 2022.

[18]H. -T. Nguyen and C. C. Cheah, "Analytic deep neural network-based robot control," *IEEE/ASME Trans. Mechatronics*, vol. 27, no. 4, pp. 2176-2184, Aug. 2022.

[19]S. Zhang, P. Yang, L. Kong, W. Chen, Q. Fu and K. Peng, "Neural networks-based fault tolerant control of a robot via fast terminal sliding mode," *IEEE Trans. Syst. Man Cybern. Syst.*, Aug. 2019.

[20]F. O. Karray and C. de Silva, *Soft Computing and Intelligent Systems Design,* Harlow: Pearson Higher Education, 2004.

[21]J. -S. R. Jang, C. -T. Sun and E. Mizutani, *Neuro-Fuzzy and Soft Computing,* Upper Saddle River, NJ, United States: Prentice Hall, 1997.

[22]A. Madkour, M. A. Hossain, K. P. Dahal and H. Yu, "Intelligent learning algorithms for active vibration control," *IEEE Trans. Syst. Man Cybern. Syst.*, vol. 37, no. 5, pp. 1022-1033, Sept. 2007.

[23]S. Harifi, M. Khalilian, J. Mohammadzadeh and S. Ebrahimnejad, "Optimizing a neuro-fuzzy system based on nature-inspired emperor penguins colony optimization algorithm," *IEEE Trans. Fuzzy Syst.*, vol. 28, no. 6, pp. 1110-1124, Jun. 2020.

[24]B. Selma, S. Chouraqui, B. Selma, H.Abouaïssa and T. Bakir, "Autonomous trajectory tracking of a quadrotor UAV using ANFIS controller based on Gaussian pigeon-inspired optimization,"*CEAS Aeronaut. J.*, vol. 12, pp. 69-83, Oct. 2020.

[25]M. Dorigo, V. Maniezzo and A. Colorni, "Ant system: optimization by a colony of cooperating agents," *IEEE Trans. Syst. Man Cybern.. Syst.*, vol. 26, no. 1, pp. 29-41, Feb. 1996.

[26]R. Frank, *Understanding Smart Sensors*, Boston, MA, United States: Artech House, 2013

[27]W. Wang, "An intelligent system for machinery condition monitoring," in *IEEE Trans. Fuzzy Syst.*, vol. 16, no. 1, pp. 110-122, Feb. 2008.

[28]S. G. Kelly, *Mechanical Vibrations: Theory and applications*, Australia: Cengage Learning, 2012.

[29]M. S. Allen, H. Sumali and D. S. Epp "Piecewise-linear restoring force surfaces for semi-nonparametric identification of nonlinear systems," in *Nonlinear Dyn.*, vol. 54, pp. 123-135, 2008.

Adam Genno received his Advanced Diploma in Electromechanical Engineering Technology from Humber College (Etobicoke, Ontario, Canada) in 2013. He received the B.Eng. degree in Mechanical Engineering from Lakehead University (Thunder Bay, Ontario, Canada) in 2020 He is currently working toward the M.S. degree in Mechanical Engineering at Lakehead University.

From 2013 to 2019 he worked as a Machine Vision Technologist at Vista Solutions Inc. (Windsor, Ontario) and a Quality Engineer at Honda of Canada Manufacturing (Alliston, Ontario). His research interests include intelligent control, robotics, mechatronics, artificial intelligence and machine learning.

Wilson Wang (M'04–SM'07) received his M.Eng. in Industrial Engineering from the University of Toronto (Toronto, Ontario, Canada) in 1998 and Ph.D. in Mechatronics Engineering from the University of Waterloo (Waterloo, Ontario, Canada) in 2002, respectively.

From 2002 to 2004, he was employed as a senior scientist at Mechworks Systems Inc. He joined Lakehead University in 2004, and now he is a professor in the Department of Mechanical Engineering. His research interests include mechatronics, artificial intelligence, machine learning, diagnostics and prognostics of engineering systems, smart sensors, intelligent control, and signal processing. Besides teaching and research, he has contributed to several journal boards and organizations, for example, the Chair of Expert Committee for CFI (Canada Foundation for Innovation) 2021-2023.